Communication

In Situ Detection of the Flexural Fracture Behaviors of Inner and Outer Bamboo-Based Composites

Xiu Hao [1], Yanglun Yu [2], Chunmei Yang [1,*] and Wenji Yu [1,2,*]

1   College of Mechanical and Electrical Engineering, Northeast Forestry University, Harbin 150006, China
2   Research Institute of Wood Industry, Chinese Academy of Forestry, Beijing 100091, China
*   Correspondence: ycmnefu@126.com (C.Y.); yuwenji@caf.ac.cn (W.Y.); Tel.: +86-188-4515-4869 (C.Y.); +86-010-8288-9427 (W.Y.)

Abstract: This paper investigated the fracture toughness and enhancement mechanism for each component in bamboo-based composites at the cellular level. In situ characterization techniques identified the fracture behaviors of bamboo-based composites in three-point bending tests, and scanning electron microscope (SEM) further visualized the crack propagation of the fracture surface. In addition, the improvement mechanism of bamboo-based composites was illustrated by mechanical properties at the cellular level assisted with nanoindentation tests. Our in situ test results showed that the bamboo-based composites exhibited a longer deformation and higher bending load compared with bamboo. The fracture was non-catastrophic, and crack propagated in a tortuous manner in bamboo-based composites. Microstructural analysis revealed that phenol-formaldehyde (PF) resin pulled out and middle lamella (ML) breaking rather than transverse transwall fracturing occurred in parenchymal cells. The higher density of fibers in the bamboo-based composites triggered massive interfacial delamination in the middle lamella (ML), which was a weak mechanical interface. Furthermore, indented modulus and hardness illustrated that phenol-formaldehyde (PF) resin improved the mechanical strength of cell walls, especially parenchymal cells. The crosslinks of PF resin with the cell walls and massive fibers were the primary mechanisms responsible for the fracture toughness of bamboo-based composites, which could be helpful for advanced composites.

Keywords: fracture behaviors; fibers; in situ bending tests; mechanical properties; parenchymal cells; bamboo-based composites

1. Introduction

Bamboo is a biodegradable, rapidly renewable, and high-yielding natural material on Earth [1,2]. Bamboo is composed of fiber cells, parenchymal cells, and vessels. The stiff fibers embed into the soft parenchyma ground exhibiting remarkable mechanical strength and fracture toughness, which has traditionally been used in the building industry, such as flooring, roofing, walls, and scaffolding [3,4]. However, bamboo is highly variable in mechanical properties owing to its hollow structure [5,6]. These unique characteristics require great attention to bamboo-based panels or engineered products (bamboo plywood, laminated bamboo lumber, bamboo particleboard, bamboo scrimber), in which component preparation and adhesives bonding are critical to the manufacturing process to reduce the environmental load [7,8]. Bamboo is a natural functional hierarchical structure material composed of orientated stiff fibers and a soft parenchyma matrix [9–11]. At a macroscopic scale, vascular bundles display a decisive role in the mechanical properties of bamboo; however, the parenchyma tissues contribute to transferring the stress. At the microscopic level, fiber cell walls have a multilayered wall structure with a tiny lumen, and the parenchymal cells have a thin wall and larger lumen [12–17]. Getting a deep study on the improvement mechanism of different components in the bamboo-based panel could be helpful in designing biomimetic polymeric composites.

More research efforts have been made recently in studying the mechanical properties and toughness mechanism by observing the fracture behavior of the hierarchical structure in bamboo with the assistance of in situ mechanical testing, particularly at the cellular level [18,19]. Among these efforts, most studies indicated that fiber gradient distribution and parenchymal tissue displayed different fracture behavior under bending tests [9,10]. Parenchymal cells were weak points [18]; however, the oriented stiff fibers were attributed to inhibiting crack growth as the bamboo fractured [19].

Bamboo scrimber is composed of bamboo fibers arranged in parallel with adhesive, showing excellent strength and quality by condensation of fiber and bonding resin [20–35]. The study focused on investigating the structure–property relationships in the bamboo scrimber. To preserve the morphology of fibers and parenchymal cells, the bamboo-based composites in this study were prepared by the inside and outside thin bamboo strips. Specially, we focus on the bending performance and fracture toughness of bamboo-based composites. In situ bending tests were conducted to prevent the fracture behaviors of bamboo-based composites. In addition, the fracture characteristics were observed by Field-emission scanning electron microscope (SEM). Finally, nanoindentation tests were used to illustrate the mechanical properties at the cellular level.

2. Materials and Methods
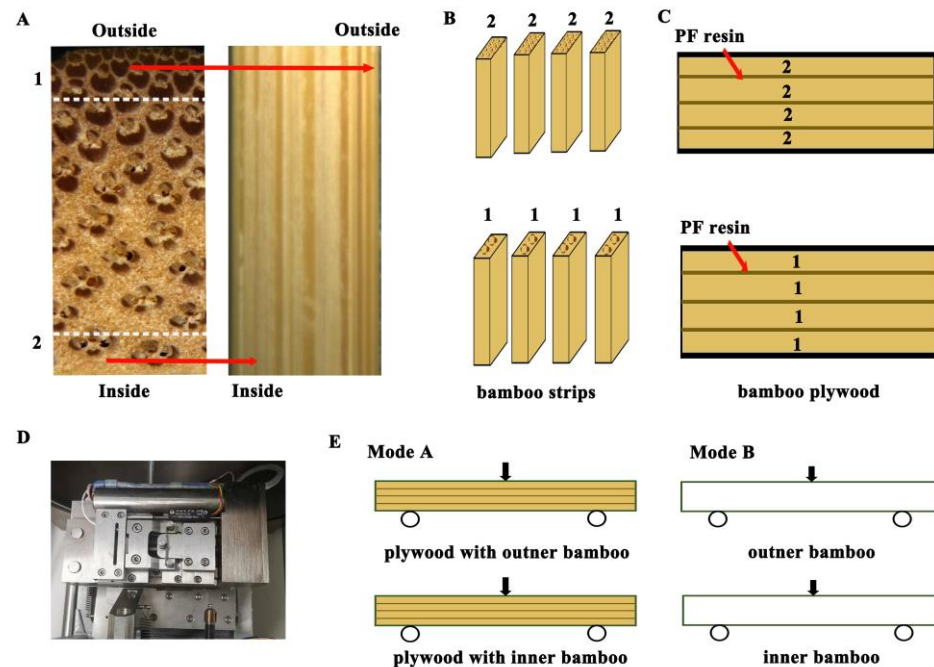
2.1. Samples Preparation

The 4 years old moso bamboo (*Phyllostachys pubescens* Mazel ex H.de Lehaie) was collected from Zhejiang province in China for this study. The bamboo wall was 8–10 mm thick, and the diameter at breast height was 120 mm. Samples were taken from the internodes located at the culm height of 2 m. Then, the specimens were kept in an environment of 65% relative humidity and a conditioning chamber (25 °C) until an EMC of 10%–12%.

The distribution of vascular bundles in bamboo followed a gradually increased order from the inner to the outer part along the radial direction showing a hierarchical characteristic, as presented in Figure 1A. Bamboo was sliced into two pieces of ~1 mm thickness strands from the inner and outer parts (Figure 1B) to prepare the bamboo-based composites made from the different zone of the bamboo portion. The densities of inner and outer bamboo were 0.65 g/cm^3 and 0.9 g/cm^3, respectively. The making process of bamboo-based composites was as follow: firstly, the bamboo strips from the inner and outer part with a dimension of 100 (l) $\times$ 10 (t) $\times$ 1 (r) mm^3 were immersed in a 15% aqueous solution PF resin for 12 h. Then, samples were kept under ambient conditions for 12 h and were then oven dried at 50 °C for 2 h. After oven drying, the specimens were conditioned at 60% relative humidity (20 °C) to regulate moisture content. Four oven-dried resin-impregnated specimens of each part were parallel glued and pressed at 150 °C under 3 MPa to obtain bamboo-based composites with a dimension of 100 (l) $\times$ 10 (t) $\times$ 2 (r) mm^3 (Figure 1C), and the density of bamboo-based composites is 1.10–1.15 g/cm^3. The specimens were kept in an environment of 60% relative humidity and a conditioning chamber to EMC of 10%–12%.

2.2. In Situ Mechanical Tests

The in situ bending tests were conducted in an SEM chamber (Quanta 2000, FEI, Hillsboro, OR, USA) with a miniature mechanical testing device (Microtest 2000, Deben Ltd., East Grinstead, UK) equipped with a maximum load capacity of 660 N (Figure 1D). For the three-point bending tests, five samples were cut from the middle of the scrimber (Figure 1E). The inner and outer parts of bamboo were also obtained as a control group (Figure 1E). Then, the samples were polished by a sliding microtome. The dimension of inner bamboo, outer bamboo, and bamboo-based composites was 30 (l) $\times$ 2 (t) $\times$ 4 (r) mm^3, 30 (l) $\times$ 2 (t) $\times$ 4 (r) mm^3, and 30 (l) $\times$ 2 (t) $\times$ 2 (r) mm^3 to obtain the load–displacement curves. To obtain the microscopic images with equal precision, the dimension of inner bamboo, outer bamboo, and bamboo-based composites was 30 (l) $\times$ 2 (t) $\times$ 2 (r) mm^3. The three-point bending tests were conducted according to the Chinese standard of GB/T 15780-1995 and the fracture process of the samples during bending tests was examined in

real-time. The crack initiation and propagation mechanism in bamboo-based composites and bamboo could be characterized simultaneously by the SEM images. The in situ tests were taken at room temperature with an acceleration voltage of 5 kV.

Figure 1. Schematic of test samples preparation. (**A**) images of bamboo culm; (**B**) bamboo strips from the inside and outside; (**C**) bamboo-based composites; (**D**) bending tests; (**E**) flexural bending configures of bamboo-based composites (mode A) and bamboo strips (mode B).

2.3. Morphology Characterization

Bending-induced fracture appearances of specimens were produced by a field-emission scanning electron microscope (SEM, Hitachi, S-4800,Tokyo, Japan). Five specimens with a dimension of 5 (l) $\times$ 2 (t) $\times$ 2 (r) mm^3 were plated with gold, and the acceleration voltage was 10 kV. The SEM experiments were operated at ambient conditions.

2.4. Nanoindentation and Dynamic Modulus Analysis

The nanoindentation and dynamic modulus maps tests (Hysitron TI 980 TriboIndenter, Bruker, Germany) measured the mechanical properties of the cell walls in the bamboo-based composites. Five samples with a size of 5 (l) $\times$ 1 (r) $\times$ 1 (t) mm^3 were prepared by grinding and polishing to obtain a smooth surface. The Berkovich tip was loaded to a 10 mN peak at a 20 uN·s^{-1} rate and then held at a constant load for 5 s. The hardness and reduced elastic modulus were calculated from the positions on each wall layer and middle lamellae (ML) in fiber cells and parenchymal cells in bamboo-based composites. After indentation, the in situ scanning probe microscopy images observed the indents' position and morphological characteristics. The nanoindentation tests were taken at room temperature.

3. Results

3.1. The Fracture Behavior of Inner Bamboo-Based Composites

The load–displacement curves for in situ bending tests of bamboo-based composites from inner bamboo and the inner part of bamboo were plotted in Figure 2. The results revealed that the fracture of bamboo-based composites during bending was non-catastrophic and more complicated than the failure of bamboo. The bending force in bamboo-based composites with 1.15 g/cm^3 was ~50 N, which was higher than that of bamboo with 0.65 g/cm^3.
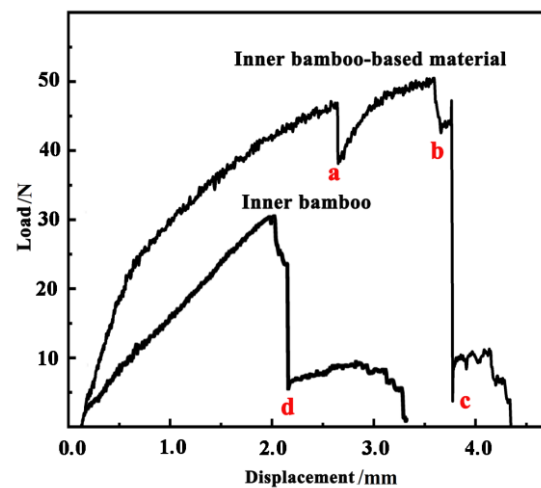
Figure 2. The represented load–displacement curves and loading stage for in situ bending tests on the specimens from the inner bamboo-based composites (a–c) and the inner bamboo (d).

A serious of SEM images corresponding to the bending strain detected by in situ tests were also shown in Figure 3. As shown in Figure 3B, the initial cracks occurred in the outer of the bamboo-based composites, and the cracks propagated across the parenchyma tissue in a tortuous manner, which was accompanied by the first load drop (a) in Figure 2. In the following process, the cracks reached fiber bundles and deviated from the initial direction to the interface of fiber bundles. Once the cracks induce dramatic interface delamination of fibers, the cracks developed in the parenchymal tissues on the side of the fiber, which also showed a tortuous route, where the loading was indicated by points b–c. In accordance with the in situ snapshots in Figure 3C, parenchymal tissue fracture and interfacial failure were the dominant fracture mode in the bamboo-based composites. Meanwhile the inner part of the bamboo failure displayed almost a brittle fracture, as indicated by points d in Figure 2. The visible cracks initiated quickly within the bottom area in the parenchyma cells (Figure 3E), which sharply propagated and resulted in a transverse wall failure of the parenchymal tissues (Figure 3F).
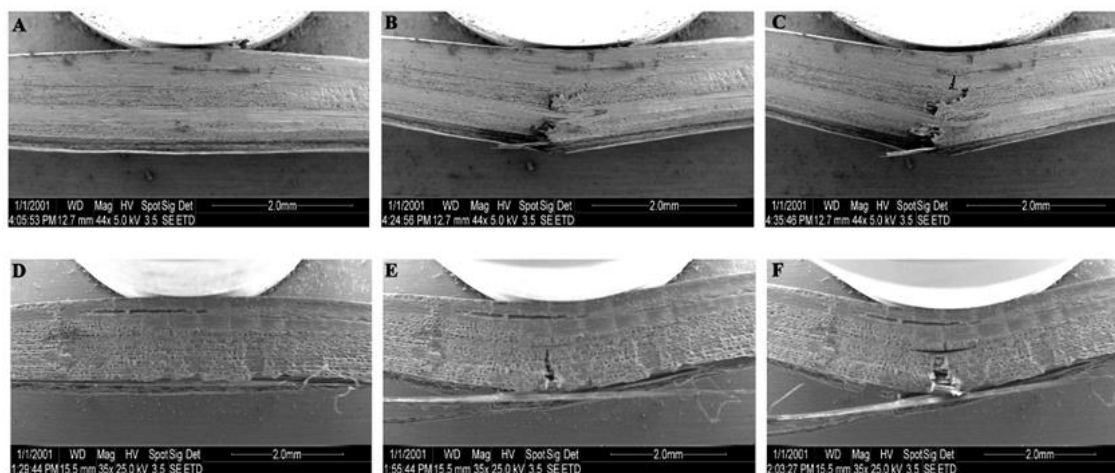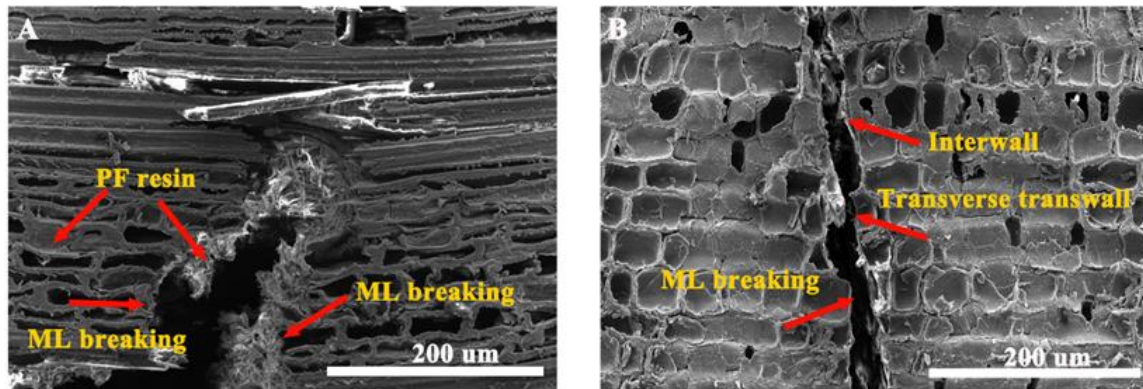

Figure 3. In situ three-point bending tests of the inner bamboo-based composites (**A**–**C**) and the inner bamboo (**D**–**F**).

Figure 4 further presents SEM images of the fracture surfaces and crack growth of failure samples. According to the microstructure in Figure 4A, the bamboo-based composites displayed almost ML breaking and pullout of the PF resin, exhibiting a rough fracture surface. In addition, the crack propagated along the ML interface of parenchymal

cells in a tortuous manner. Meanwhile, SEM images in Figure 4B illustrated that repeated ML breaking and transverse wall of parenchyma cells were the most prominent feature in the inner bamboo fracture surface with a straight fracture path. This could be PF resin filled in the parenchymal cells and crosslinked with the cell wall and improved the mechanical properties of cell walls. Therefore, the PF resin could help dissipate the stress and prevented the parenchymal cells from failing.

Figure 4. SEM images of three-point bending tests of the inner bamboo-based composites (**A**) and inner bamboo (**B**).

3.2. Fracture Behavior of Outer Bamboo-Based Composites

In this study, the simultaneous detection of load–displacement behaviors of the bamboo-based composites from outer bamboo and the outer bamboo is shown in Figure 5. According to the results, the bamboo-based composites exhibited a long deformation with a maximum load of ~80 N, while the samples of bamboo indicated a short elongation with a maximum load of ~40 N. During the bending process, the bending behaviors of bamboo-based composites were more complicated, displaying a stepwise fracture process from the higher force field (point a) to the lower force field (point d).
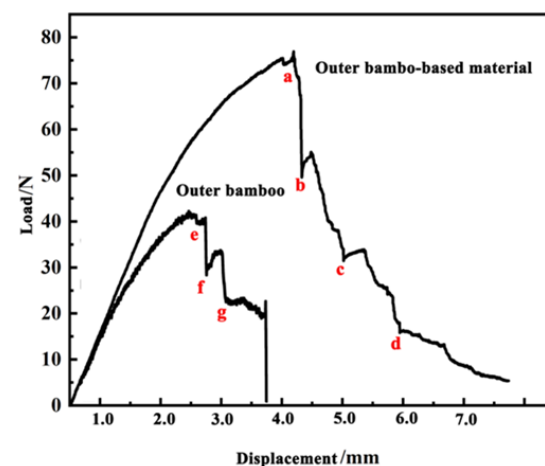
Figure 5. The represented load-displacement curves and loading stage for in situ bending tests on the specimens from the outer bamboo-based composites (a–d) and the outer bamboo (e–g).

Figure 6 presents a series of SEM images of the instant crack initiation and propagation process of the specimens in bending tests, corresponding to the various stages in Figure 5. At first, when the bending load reached the maximized value, visible cracks were initiated and occurred in the bottom area of the bamboo-based composites, which sharply propagated to the closer fiber layer (Figure 6B), and an obvious yield point (a) took place in the load–displacement curve as shown in Figure 5. Afterward, the closest fiber obstructed the crack

extension, and the crack tip propagated along the interface of the fiber bundles, which induced debonding of the fibers (Figure 6C). In the following process, the stiff fiber bundles bore a high load, which resulted in the repeated process of crack propagating and interface delamination with further increasing loading (Figure 6D). The cracks propagated in a layer-by-layer path resulting in successive drop load from point a to b (Figure 5). Furthermore, the bamboo-based composites with a higher density of fiber bundles were able to sustain the higher bending loads.
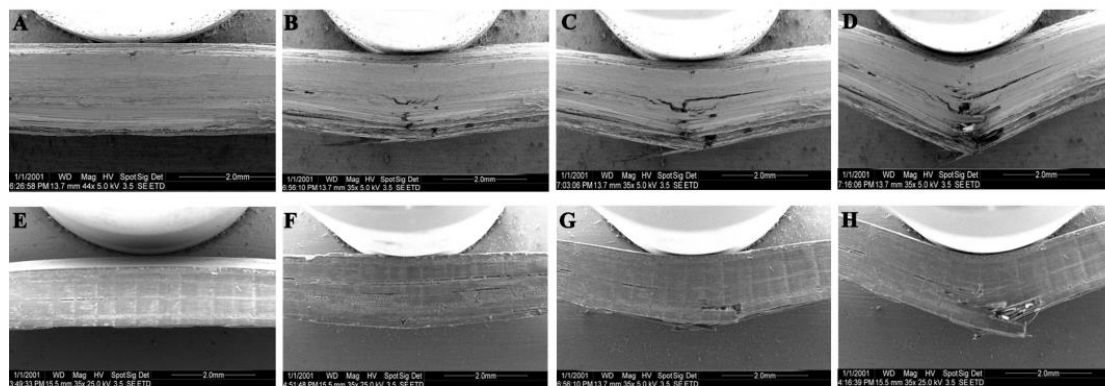
Figure 6. In situ three-point bending tests of the outer bamboo-based composites (**A**–**D**) and the outer bamboo (**E**–**H**).

In the case of bamboo (Figure 6E), the initial cracks occurred in the bottom (Figure 6F) and propagated perpendicular to the closest fiber layer (Figure 6G), which triggered a drop from point e to g in Figure 5. In the flowing process, the cracks also resulted in interface delamination in the fiber bundles (Figure 6H). The results showed that the degree of deformation in bamboo-based composites was obviously larger than that in outer bamboo, which can be attributed to more fiber density.

To further visualized the crack growth mode, Figure 7 showed the SEM images of the bamboo-based composites and the outer part of bamboo specimens in bending. Micro-structural images presented in Figure 7A revealed that the bamboo-based composites with higher fibers exhibited longitudinal crack propagation, and the stiff fiber bundles obstructed crack tip growing by fiber bridging and ML breaking, resulting in interface delamination. In addition, the fiber bundles displayed a rough fracture appearance attributed to PF resin coating. By contrast, the bending tests of bamboo with lower fiber triggered more fiber failure displaying fiber pullout and bridging (Figure 7B). Compared with crack propagation in the outer of the bamboo, the influence of higher fiber and PF resin in bamboo-based composites blunted the transverse crack growth.
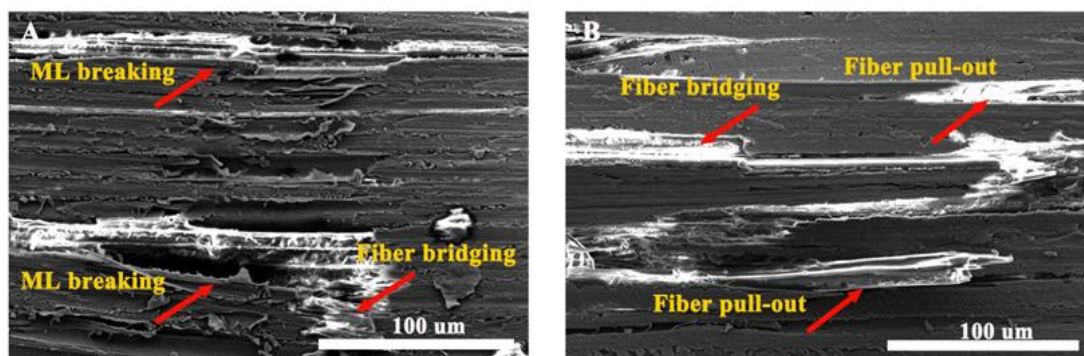
Figure 7. Micro-images of the outer bamboo-based composites (**A**) and the outer bamboo (**B**).

3.3. Micro-Mechanical Properties of Cell Walls in Bamboo-Based Composites

Reduced modulus and hardness were obtained to investigate the mechanical properties of fiber and parenchymal cells in bamboo-based composites, which were showed in Figure 8. In the fiber and parenchymal cells of bamboo-based composites, the structural difference in cell wall layers resulted in the reduced modulus and hardness values varying from the secondary cell wall to ML corresponding to bamboo. The storage modulus of the s2, s1, and ML layers in the fiber cell was 27 GPa, 24 GPa, and 18 GPa, respectively, which were higher than that in bamboo in our previous study [15]. Furthermore, the storage modulus of the parenchymal cell walls and ML layer was 15 GPa and 13 GPa in the bamboo-based composites, which were more than those in bamboo. The hardness in the fibers (s2: 0.78 GPa, s1: 0.66 GPa, ML: 0.67 GPa) and parenchymal cells (s: 0.66 GPa, ML: 0.64 GPa) also exhibited increment compared to that in bamboo. These results may be due to the cross-linking reaction between PF resin and cell walls in fiber and parenchymal cells, which improved the mechanical strength of cell walls. Comparing with the mechanical strength values of fiber and parenchyma cells, it was found that the increment rate of indentation modulus and hardness values of parenchyma cells was greater than that of fiber cells, which indicated more PF resin permeating in the cell walls in parenchymal cells. Hence, cell wall failure of parenchymal cells in the bamboo-based composites occurred an ML and PF resin breaking rather than transverse transwall fracture. Meanwhile, as shown in Figure 8, the storage modulus of the ML in fiber and parenchyma cells was lower than those of the cell walls, which were the weak interface in the bamboo-based composites. Hence, interface delamination of fibers and ML-PF resin pullout in parenchymal cells were the prominent fracture characteristic in the bamboo-based composites. While compared with the fiber cells, the reduced modulus value of the s layer in parenchymal cells was much lower than that in fiber cell walls. This may be accounting for the fiber cells being the strongest interface in graded bamboo structure, which prevented fiber cells from bucking under the external force.
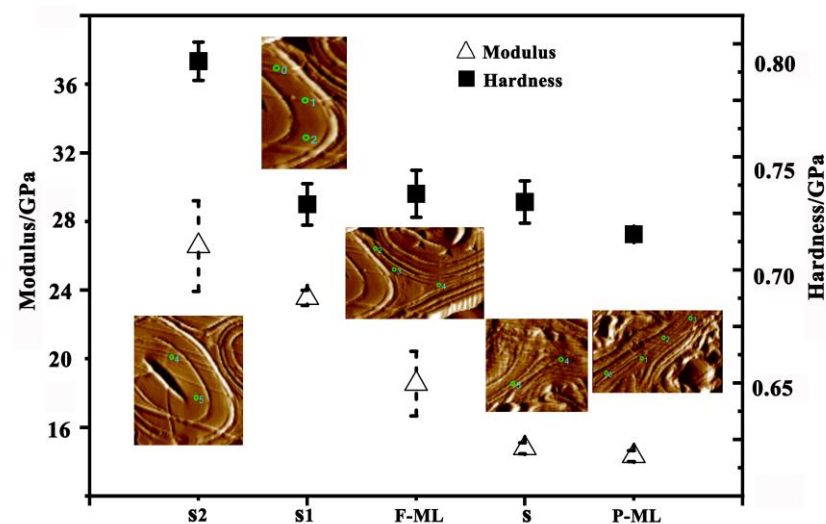
Figure 8. The modulus and hardness of the fiber and parenchymal cell walls and different layers in bamboo-based composites (s2, s1: Fiber cell wall; F-ML: ML in fiber cell; s: Parenchymal cell wall; P-ML:ML in parenchymal cell; 0–5: nanoindentation test number in fiber cells and parenchymal cells).

4. Discussion

Bamboo scrimber is prepared by bonding bamboo trips with PF resin, which show well quality and strength compared with natural bamboo. A lot of attempts have been made to illustrate the preparation and physical and mechanical properties of bamboo scrimber. Meanwhile, very few studies focused on the improvement mechanism within bamboo scrimber, especially at the cellular level. In situ detection of the fracture behaviors of moso bamboo in bending tests illustrated that the synergistic effects of the fiber bundles

and parenchyma ground played an important role in restraining crack propagation, which was mainly responsible for the fracture toughness of bamboo [17,21]. In this study, we performed in situ bending tests to directly observe the flexural response of the structural components in bamboo-based composites. Since the fiber density increases from the inside to the outside of the bamboo stem, the bamboo-based composites were composed of thin inner and outer bamboo strips arranged in parallel with adhesive in this work to get an understanding of the fracture behavior of the fiber and parenchymal cells. The load–displacement curves revealed that inner and outer bamboo-based composites owned higher fracture loads than that of natural bamboo. The failure load of inner bamboo-based composites was two times that of inner bamboo. Compared with inner bamboo, the failure process of inner bamboo-based composites was complicated, and the load–displacement curve showed stepwise. The cured PF resin restrained the vertical crack propagation as it acted in the inner bamboo, and it triggered the peeling and delamination of parenchymal cell walls in the inner bamboo-based composites, which extended the crack growth path. Compared with the outer bamboo, the fracture load of outer bamboo-based composites increased with the fiber bundle density increasing. As the load increased, the fiber bundles were peeled off from the outer layer to the inner layer until the composite was completely destroyed, and the crack propagation path showed a zigzag crack growth mode, which was similar to the fracture behaviors of bamboo [15,17]. Meanwhile, in the in situ bending tests of outer bamboo-based composites, the fiber bundles with cured PF resin restrained crack propagation, and the fiber bundles mainly acted as interfacial debonding and fiber bridging, which showed few fiber bundle pull-out compared with the outer bamboo. As shown in a series of in situ bending tests, the bamboo-based composites exhibited distinct asymmetric crack propagation manners induced by the fiber and parenchymal cells as they acted in the bending-induced fracture behavior of bamboo in the previous study [14,15,17,19]. In this work, the cured PF resin exhibited a significant effect on crack propagation in fibers and parenchyma cells. The crack propagation behaviors in bamboo-based composites from inner bamboo showed that cracks generally occurred in the ML layer and PF resin, which caused the peeling of the parenchymal cells and the tearing of the PF resin. Crack propagation behaviors within bamboo-based composites made of outer bamboo showed that the fiber bundles played an important role in restraining crack propagation, acting as crack stoppers. In situ bending tests and the SEM micro-images illustrated the fracture toughness attributed to the higher fiber density and PF resin crosslink with the cell wall in fiber cells and parenchymal cells.

The nanoindentation characterization was conducted on the cell wall layer and ML layer in the fiber cells and parenchymal cells. The elastic modulus of bamboo presented a peak in the s2 (23.52 GPa) and declines in s1 (18.02 GPa), ML (15.91 GPa), and lumen (14.63 GPa), in that order [22]. The elastic modulus in the parenchymal cell layers exhibited a downward trend of s (10 GPa) and ML (5.57 GPa) [22]. The storage in the fiber cells (s2: 27 GPa, s1: 24 GPa, ML: 18 GPa) and (s: 15 GPa, ML: 13 GPa) parenchymal cells within bamboo-based composites exhibited higher values compared to natural bamboo. We confirmed that fibers were indeed the strongest phase and ML was comparatively weaker, while PF resin improved the mechanical properties of cell wall layers in bamboo. By learning from the cellular structure of bamboo-based composites during real-time bending deformation, it is possible to reveal the structure–property relationships of bamboo-based composites and could be helpful in understanding and designing the advanced biological composites.

5. Conclusions

In summary, the bamboo-based composites exhibited greater fracture toughness than bamboo, showing a longer deformation and less damage to fiber and parenchymal cell walls. The improvement mechanism was highly attributed to the reaction of PF resin with cell walls and fiber density. In situ bending tests and SEM observing of bamboo-based composites from inner bamboo illustrated that cracks generally occurred in the ML layer

and PF resin, which caused the peeling of the parenchymal cells and the tearing of the PF resin. The cracks propagated in a tortuous manner, leading to massive interfacial debonding rather than transverse transwall fracture behavior for parenchymal cell walls in bamboo-based composites.

Crack propagation behavior within bamboo-based composites made of outer bamboo showed that the fiber bundles played an important role in restraining crack propagation, acting as crack stoppers. More fiber bundles in the bamboo-based composites trigged massive interfacial delamination, exhibiting ML breaking and fiber bridging. The cracks propagated in a zigzag manner within the fiber bundles under bending, leading to interfacial delamination. The occurrence of parenchymal cell pealing, PF resin tearing, and interfacial delamination was regarded as dissipating the crack energy.

Nanoindentation tests were conducted to reveal the improvement mechanism of fiber and parenchymal cell walls. The fiber cell and parenchymal cells within bamboo-based composites exhibited higher storage modulus compared to natural bamboo, which indicated that the PF resin improved the mechanical properties of fiber and parenchymal cells in bamboo-based composites. The effects of PF resin were regarded to be mainly responsible for preventing cell walls from destruction, especially parenchymal cells.

Author Contributions: X.H.: Data curation, Investigation, Writing—original draft. Y.Y.: Formal analysis. C.Y.: supervision, Writing—review and editing. W.Y.: Conceptualization, Funding acquisition, Methodology, Project administration. All authors have read and agreed to the published version of the manuscript.

Data Availability Statement: All relevant data are within the paper.

References

1. Lugt, V.; Dobbelsteen, V.D. An environmental, economic and practical assessment of bamboo as a building material for supporting structures. *Constr. Build. Mater.* **2006**, *20*, 648–656. [CrossRef]
2. Li, Y.; Xu, b.; Zhang, Q. Present situation and the countermeasure analysis of bamboo timber processing industry in China. *J. For. Eng.* **2016**, *1*, 2–7. (In Chinese)
3. Sharma, B.; Gatoo, A.; Bock, M. Engineered bamboo for structural applications. *Constr. Build. Mater.* **2015**, *81*, 66–73. [CrossRef]
4. Wu, B.; Gatoo, A.; Bock, M. Engineered bamboo for structural applications. *J. Nanjing For. Univ. (Nat. Sci. Ed.).* **2014**, *38*, 115–120. (In Chinese)
5. Qi, J.; Xie, J.; Huang, X.; Yu, W.; Chen, S. Influence of characteristic inhomogeneity of bamboo culm on mechanical properties of bamboo plywood: Effect of culm height. *J. Wood. Sci.* **2014**, *60*, 396–402. [CrossRef]
6. Zhan, T.; Sun, F.; Chao, L. Moisture diffusion properties of graded hierarchical structure of bamboo: Longitudinal and radial variations. *Constr. Build. Mater.* **2020**, *259*, 119641. [CrossRef]
7. Nogata, F.; Takahashi, H. Intelligent functionally graded material: Bamboo. *Composites.* **1995**, *5*, 743–751. [CrossRef]
8. Nkeuwa, W.; Zhang, J.; Semple, K.; Chen, M.; Xia, Y.; Dai, C. Bamboo-based composites: A review on fundamentals and processes of bamboo bonding. *Composites* **2022**, *235*, 109776. [CrossRef]
9. Dixon, P.G.; Gibson, L.J.; Bock, M. The structure and mechanics of moso bamboo material. *Sci. Rep.* **2014**, *11*, 20140321. [CrossRef]
10. Wang, X.; Ren, H.; Zhang, B.; Fei, B.; Burgert, I. Cell wall structure and formation of maturing fibres of moso bamboo (Phyllostachys pubescens) increase buckling resistance. *J. R. Soc. Interface* **2012**, *9*, 988–996. [CrossRef]
11. Lian, C.; Liu, R.; Zhang, S.; Yuan, J.; Luo, J.; Yang, F.; Fei, B. Ultrastructure of parenchyma cell wall in bamboo (Phyllostachys edulis) culms. *Cellulose* **2020**, *27*, 7321–7329. [CrossRef]
12. Parameswaran, N.; Liese, W. On the fine structure of bamboo fibres. *Wood Sci. Technol.* **1976**, *10*, 231–246. [CrossRef]
13. Shao, Z.; Fang, C.; Huang, S. Tensile properties of moso bamboo (Phyllostachys pubescens) and its components with respect to its fiber-reinforced composite structure. *Wood Sci. Technol.* **2010**, *44*, 655–666. [CrossRef]
14. Habibi, M.; Lu, Y. Cracks propagation in bamboo's hierarchical cellular structure. *Sci. Rep.* **2014**, *4*, 5598. [CrossRef] [PubMed]
15. Liu, H.; Wang, X.; Zhang, X.; Sun, Z.; Jiang, Z. In situ detection of the fracture behaviour of moso bamboo (phyllostachys pubescens) by scanning electron microscopy. *Holzforschung* **2016**, *70*, 1183–1190. [CrossRef]
16. Wang, F.; Shao, Z.; Bock, M. Study on the variation law of bamboo fibers' tensile properties and the organization structure on the radial direction of bamboo stem. *Ind. Crops Prod.* **2020**, *152*, 112521. [CrossRef]

17. Wang, D.; Lin, L.; Fu, F. Fracture mechanisms of moso bamboo (*Phyllostachys pubescens*) under longitudinal tensile loading. *Ind. Crops Prod.* **2020**, *153*, 112574. [CrossRef]

18. Obataya, E.; Kitin, P.; Yamauchi, H. Bending characteristics of bamboo (Phyllostachys pubescens) with respect to its fiber–foam composite structure. *Wood Sci. Technol.* **2007**, *41*, 385–400. [CrossRef]

19. Chen, M.; Ye, L.; Wang, G.; Fang, C.; Dai, C.; Fei, B. Fracture modes of bamboo fiber bundles in three-point bending. *Cellulose* **2019**, *26*, 8101–8108. [CrossRef]

20. Hao, X.; Tian, X.; Li, S.; Yang, C.; Yu, Y.; Yu, W. The separation mechanism of bamboo bundles at the cellular level. *Forests* **2022**, *13*, 1897. [CrossRef]

21. Yu, W.; Yu, Y. Development and prospect of wood and bamboo scrimber industry in China. *China Wood Ind.* **2013**, *27*, 5–8. (In Chinese)

22. Zhang, Y.; Huang, Y.; Zhang, Y.; Yu, Y.; Yu, W. Scrimber board (sb) manufacturing by a new method and characterization of sb's mechanical properties and dimensional stability. *Holzforschung* **2018**, *72*, 283–289. [CrossRef]

23. Wei, J.; Rao, F.; Zhang, Y.; Li, C.; Yu, W. Effect of veneer crushing process on physical and mechanical properties of scrimbers made of pinus radiata and populus tomentosa. *China Wood Ind.* **2019**, *33*, 55–58. (In Chinese)

24. Yu, Y. Manufacturing technology and mechanism of high performance bamboo-based fiber composites. Ph.D. Thesis, Chinese Academy of Forestry, Beijing, China, 2014. (In Chinese).

25. Bao, M.; Huang, X.; Zhang, Y.; Yu, W.; Yu, Y. Effect of density on the hygroscopicity and surface characteristics of hybrid poplar compreg. *Wood Sci. Technol.* **2016**, *62*, 441–451. [CrossRef]

26. Li, J.; Wu, Z.; He, S.; Huang, C.; Chen, Y. Effect of bundle diameter on water absorption properties of bamboo scrimber. *J. Zhejiang For. Sci. Technol.* **2016**, *36*, 67–70. (In Chinese)

27. Li, Q.; Wang, K.; Yang, W.; Hua, X.; Weng, F.; He, Q. Research on technology of remaking bamboo glued board. *J. Bamboo. Re.* **2003**, *22*, 56–60. (In Chinese)

28. Fu, Y.; Fang, H.; Dai, F. Study on the properties of the recombinant bamboo by finite element method. *Composites* **2017**, *115*, 151–159. [CrossRef]

29. Kumar, A.; Vlach, T.; Laiblova, L. Engineered bamboo scrimber: Influence of density on the mechanical and water absorption properties. *Constr. Build. Mater.* **2016**, *127*, 815–827. [CrossRef]

30. Li, Z.; Chen, C.; Mi, R.; Gan, W.; Dai, J.; Jiao, M.; Xie, H.; Yao, Y.; Xiao, S.; Hu, L. A Strong, Tough, and Scalable Structural Material from Fast growing Bamboo. *Adv. Mater.* **2020**, *32*, 1906308. [CrossRef]

31. Yu, Y.; Liu, R.; Huang, Y.; Meng, F.; Yu, W. Preparation, physical, mechanical, and interfacial morphological properties of engineered bamboo scrimber. *Constr. Build. Mater.* **2017**, *157*, 1032–1039. [CrossRef]

32. Yu, Y.; Huang, X.; Yu, W. A novel process to improve yield and mechanical performance of bamboo fiber reinforced composite via mechanical treatments. *Composites* **2014**, *56*, 48–53. [CrossRef]

33. Meng, F. Study on the bonding interface and mechanism of bamboo-based fiber composites. Ph.D. Thesis, Beijing Forestry University, Beijing, China, 2017. (In Chinese).

34. Shams, M.; Kagemori, N.; Yano, H. Compressive deformation of wood impregnated with low molecular weight phenol formaldehyde (PF) resin IV: Species dependency. *J. Wood Sci.* **2006**, *52*, 179–183. [CrossRef]

35. Wang, X.; Luo, X.; Ren, H. Bending failure mechanism of bamboo scrimber. *Constr. Build. Mater.* **2022**, *4*, 326. [CrossRef]